Evaluation of magnetic resonance imaging for detection of internal tumors in green turtles with cutaneous fibropapillomatosis

Lara A. Croft, DVM; John P. Graham, MVB, MSc; Susan A. Schaf, BS; Elliott R. Jacobson, DVM, PhD

Objective—To describe the gross cross-sectional anatomy of green turtles (*Chelonia mydas*) and evaluate magnetic resonance imaging (MRI) for detection of internal tumors in green turtles with cutaneous fibropapillomatosis.

Design—Prospective study.

Animals—3 dead green turtles, 1 healthy green turtle, and 8 green turtles with cutaneous fibropapillomatosis.

Procedures—Gross cross-sectional anatomy of a dead turtle was described. Each live turtle underwent a complete physical examination, and dorsoventral whole-body survey radiographic views were obtained. Magnetic resonance imaging was performed in dorsal and transverse planes. Radiographs and magnetic resonance images were examined for evidence of internal nodules. Results were compared with necropsy findings in 5 of 8 turtles.

Results—Nodules in the lungs of 2 turtles were detected via radiography, whereas pulmonary nodules were detected in 5 turtles via MRI. No other visceral nodules were detected via radiography; however, masses in the stomach and adjacent to the bladder and kidneys were detected in 1 turtle via MRI. Other extrapulmonary abnormalities observed at necropsy were not detected on MR images.

Conclusions and Clinical Relevance—MRI may be valuable for detection of internal tumors in green turtles with cutaneous fibropapillomatosis. Nodules were more apparent in the lungs than in other organs. Results of MRI may serve as prognostic indicators for sea turtles undergoing assessment, treatment, and rehabilitation. Clinical application may be limited by cost and availability of MRI technology. (*J Am Vet Med Assoc* 2004;225:1428–1435)

WILDLIFE

Fibropapillomatosis is a common disease of wild-caught green turtles living in many areas of the world; the disease has also been recognized in other species of marine turtles.[1] In certain areas, the prevalence of fibropapillomatosis is high; results of a survey conducted in the 1980s indicated that > 50% of some populations of green turtles were affected in certain regions of Florida and Hawaii.[1] Turtles with fibropapillomatosis commonly have multiple benign cutaneous fibroepithelial tumors that are found at almost any anatomic site. Tumors can range from a few millimeters to > 20 cm in diameter.[1] Fibrous tumors (fibromas) may develop in multiple visceral sites (lungs, kidneys, liver, and gastrointestinal tract).[1] An alpha herpesvirus is suspected to be the causative agent, and although this herpesvirus has been partially sequenced, it has not been isolated in cell culture.[2]

Internal fibromas enlarge slowly, and their presence is used as a prognostic indicator for survival because they result in profound pathologic changes in affected organs or cause mechanical damage in surrounding tissues. Because of the poor prognosis, turtles with internal tumors are generally euthanatized. A diagnostic technique that allows detection of internal tumors would be of value.

Radiography is useful in chelonians for the evaluation of traumatic injuries, detection of soft tissue mineralization and foreign bodies, monitoring of bony development, and assessment of the respiratory tract.[3-5] Radiography has been used to determine the presence of internal fibromas in sea turtles with fibropapillomatosis. However, radiography is limited because soft tissue detail can be substantially obscured by the shell (carapace and plastron), which is composed of scutes that overlie ossified dermal plates.[3] In contrast, the quality of cross-sectional images such as those obtained via computed tomography and **magnetic resonance imaging (MRI)** is not affected by the shell. Magnetic resonance imaging allows for a more detailed evaluation of soft tissue structures than radiography. Few reports concerning use of MRI and computed tomography in chelonians have been published.[6] None have involved sea turtles. Considering the endangered status of most species of sea turtles, assessment of the value of diagnostic techniques, such as MRI, would help determine the best approach to diagnosis, treatment, and rehabilitation of sick or injured sea turtles. The purposes of the study reported here were to describe the cross-sectional anatomy of green turtles, evaluate MRI for the detection of internal tumors, and compare results of MRI to those obtained via radiography and postmortem examination.

Materials and Methods

Cross-sectional anatomy—One dead green turtle was frozen and sectioned in the transverse plane by use of an electric band saw. The turtle was sectioned into 1-cm-thick slices from the cranial to caudal margins of the carapace. Organs and anatomic relationships in the transverse plane were identified.

From the Department of Small Animal Clinical Sciences, College of Veterinary Medicine, University of Florida, Gainesville, FL 32610 (Croft, Graham, Jacobson); and the Turtle Hospital, 2396 Overseas Hwy, Marathon, FL 33050 (Schaf).

Supported by the Batchelor Foundation, College of Veterinary Medicine, University of Florida.

Published as University of Florida, College of Veterinary Medicine Journal Series No. 628.

The authors thank Glenn Harman and Dr. Allen Foley for assistance.

Address correspondence to Dr. Jacobson.

Turtles—One green turtle (turtle 1) obtained from an oceanarium[a] in Florida was classified as healthy on the basis of results of physical examination and absence of abnormalities on whole-body survey radiographs. This turtle underwent MRI for the purpose of establishing MRI anatomy. Slices for MRI that most closely matched the cadaveric sections were chosen. Anatomic structures were identified on magnetic resonance images via comparison with analogous structures in the cadaveric sections. Images of the coelomic cavity of 2 other stranded green turtles were used to compare dorsal MR images in corresponding planes.

Eight green turtles (turtles 2 to 9), from the Turtle Hospital in the Florida Keys, were referred to the University of Florida Veterinary Medical Teaching Hospital. These turtles were previously assessed and considered abnormal on the basis of the presence of external fibropapillomas, abnormal buoyancy, or other signs of illness. Before MRI, a complete physical examination of each turtle was performed and whole-body radiographs were obtained. Radiographs were obtained for comparison with MR images and to exclude presence of metallic objects.

All green turtles were received under the authorization of the Florida Fish and Wildlife Conservation Commission Marine Turtle Permit No. 086. For those turtles euthanatized, permission was granted by the Florida Fish and Wildlife Conservation Commission.

MRI—Approximately 20 minutes prior to the MRI procedure, turtles were sedated with ketamine (5 mg/kg [2.3 mg/lb], IM) and medetomidine (100 mg/kg [45 mg/lb], IM). When turtles were adequately sedated, they were positioned in ventral recumbency for MRI.

Magnetic resonance imaging of the healthy turtle (turtle 1) was performed by use of a commercial MRI unit.[b] Images were made in transverse and dorsal planes. A multislice acquisition technique was used, and the imaging parameters for dorsal plane T1-weighted images were **repetition time (TR)**, 693 milliseconds; **excitation time (TE)**, 20 milliseconds; slice thickness, 4 mm; **number of excitations (NEX)**, 2; for transverse plane, T1-weighted images were TR, 1,213 milliseconds; TE, 20 milliseconds; slice thickness, 5 mm; NEX, 2; and for dorsal plane, T2-weighted images were TR, 2,399 milliseconds; TE, 90 milliseconds; slice thickness, 4 mm; and NEX, 2. The field of view on images in dorsal and transverse planes was 26 × 26 cm.

Another MRI unit[c] was used to obtain images of the 8 turtles with cutaneous fibropapillomatosis. Imaging parameters for dorsal plane T1-weighted images were TR, 500 milliseconds; TE, 16 milliseconds; slice thickness, 5 to 7 mm; NEX, 1 to 3; for transverse plane, T2-weighted images were TR, 3,000 to 5,500 milliseconds; TE, 80 to 102 milliseconds; slice thickness, 10 mm; NEX, 1 to 2; for transverse plane, T1-weighted images were TR, 450 to 750 milliseconds; TE, 17 milliseconds; slice thickness, 10 mm; NEX, 1 to 2; and for dorsal plane T2-weighted images were TR, 4,000 to 5,500 milliseconds; TE, 76 to 102 milliseconds; slice thickness, 5 to 7 mm; and NEX, 2 to 3. The field of view on images in the dorsal planes ranged from 30 × 30 cm to 36 × 36 cm depending on the size of the turtle, and the field of view on transverse plane images was 16 × 16 cm to 40 × 40 cm depending on the size of the turtle or area of the turtle being scanned.

A size restriction was imposed by size of the gantry bore (60 cm in diameter) on green turtles that could be evaluated via MRI. Any turtle with a width > 60 cm would not fit into the MRI unit and therefore could not be evaluated in this study. Scans were completed in 20 to 30 minutes. All turtles with evidence of internal tumors were necropsied, and gross lesions were correlated with MR images.

Results

Cadaver anatomy—For ease of description of green turtle cross-sectional anatomy, the coelom was divided into 3 sections of equal length (cranial to caudal). A recent publication that describes the anatomy of sea turtles was used to identify anatomic structures in the cadaver.[7] The musculoskeletal, respiratory, cardiovascular, digestive, and urogenital systems were described.

Green turtles have extensive pectoral and pelvic musculature ventral to the coelomic cavity and along its entire length. The pectoral girdle musculature is comprised of a group of 5 muscles, dominated by the superficial pectoralis major, which originates on the plastron and inserts on the shaft of the humerus. This muscle group is largely responsible for respiration and locomotion. The pelvic girdle musculature is dominated by the superficial left and right rectus abdominis muscles, which originate from the lateral aspect of the pubis on each side and insert on the plastron. Skeletal muscle groups could therefore be identified on the ventral aspect of all cross-sectional slices (**Figure 1**).

The heart was located in the center of the cranial third of the coelom, caudal to the trachea and slightly cranial to the liver (**Figure 2**). The trachea bifurcated

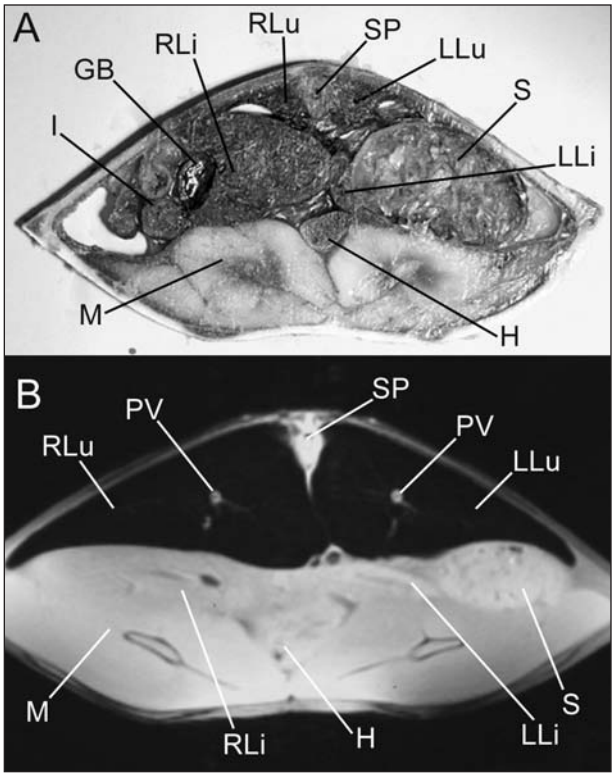

Figure 1—Photograph of a gross anatomic cross-section of the cranial portion of the coelomic cavity of a green turtle cadaver (A) and corresponding transverse plane T1-weighted magnetic resonance (MR) image of the cranial portion of the coelomic cavity of a healthy green turtle (B). The right side of the photograph and MR image correspond to the left side of the turtle, and the top of the photograph and MR image correspond to the dorsal surface of the turtle. The left lung (LLu), right lung (RLu), spine (SP), stomach (S), right liver lobe (RLi), left liver lobe (LLi), gallbladder (GB), apex of the heart (H), intestines (I), pectoral girdle musculature (M), and pulmonary blood vessels (PV) can be identified.

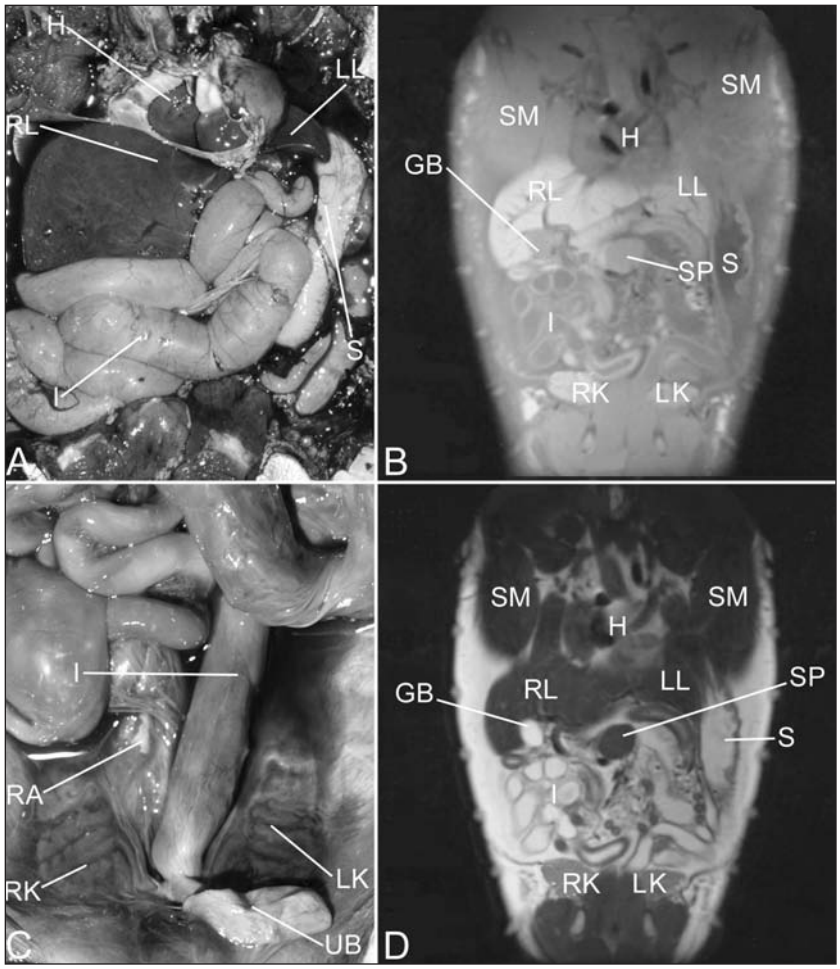

Figure 2—Photographs of gross anatomic structures in the coelomic cavity of 2 green turtle cadavers (A and C) and dorsal plane T1-weighted (B) and T2-weighted (D) MR images of the coelom, in corresponding planes, in turtle 6 that had cutaneous fibropapillomas, but no evidence of internal abnormalities via MRI. The right side of each photograph and MR image corresponds to the left side of the turtle, and the top of each photograph and MR image corresponds to the cranial end of the turtle. Notice the differences in tissue signal intensity between the T1-weighted image and the T2-weighted image. The stomach (S), right liver lobe (RL), left liver lobe (LL), gallbladder (GB), spleen (SP), intestines (I), right kidney (RK), right adrenal gland (RA), left kidney (LK), urinary bladder (UB), heart (H), and skeletal muscle (SM) can be identified.

into bronchi, and each entered 1 lung at the cranial end of the coelom; therefore, large airways were identified in cranial cross-sectional slices. Paired lungs were attached to the inner margins of the carapace, which is lined with peritoneum, and extended along the length of the coelom to the area just cranial to the hind limbs (**Figure 3**). The lungs were bilaterally symmetrical and could be seen in the dorsal portion of the coelomic cavity on all cross-sectional slices (Figure 1).

The esophagus curved in an S-shaped pattern to the left as it entered the coelomic cavity. Along the left body wall, the esophagus joined the stomach, which extended through the cranial two thirds of the coelom. The stomach was mostly on the left side of the coelom and has greater and lesser curvatures (Figure 1). The pylorus passed from left to right. The intestinal tract was long, convoluted, and distributed throughout the caudal two thirds of the coelomic cavity (Figure 2). The liver lay in the cranial to middle third of the coelom, was bilobed, and surrounded the caudal aspect of the heart. The 2 liver lobes were asymmetrical; the right lobe was much larger than the left. The gallbladder lay along the caudal surface of the dorsal right lobe of the liver. The spleen was located medial to the duodenum; however, because it is a relatively small round organ, it was not readily identified in cross-sectional slices of the cadaver specimen.

The kidneys were in the caudal third of the coelom near the caudal margins of the lungs. They were located dorsally, just beneath the carapace. The urinary bladder was located along the midline in the ventral portion of the caudal coelom (Figure 2). It was difficult to differentiate the bladder from surrounding intestines in cross-sectional slices.

MRI anatomy—The appearance of tissues on MR images is described in terms of signal intensity.[8] Tissues with a strong signal intensity appear bright or white, whereas those with low signal intensity appear dark or black with multiple shades of gray in between. The parameters used by the MRI unit to generate the images are manipulated to enhance different tissue characteristics. The most commonly used image sequences are T1- and T2-weighted. In both types of MR images, bone and cartilage are black (low signal intensity) because of their low water content. On T1-weighted MR images, fat is bright (high signal intensity), most solid organs are varying shades of gray, and fluids are dark gray. In contrast, on T2-weighted MR images, fluids and fat are bright, whereas solid tissues are varying shades of gray.

Magnetic resonance imaging provided excellent visualization of the lungs in the healthy green turtle. The lungs were black because air in the lungs does not result in an MRI signal. Branching pulmonary vasculature was best seen on dorsal plane T2-weighted images (Figure 3). The lungs were nearly symmetrical on transverse plane images and occupied almost the entire dorsal half of the body (Figure 1). On dorsal plane images, the lungs extended the length of the coelomic cavity, from the forelimbs to the hind limbs.

The heart could be identified on dorsal plane images (Figure 2). The heart had a homogeneous signal intensity that was slightly hyperintense on T2-weighted MR images compared with skeletal muscle. The gastrointestinal tract was evaluated best on dorsal plane images in which intestines could be seen in longitudinal section, and differences in wall thickness could be more readily appreciated than in other planes. Variable and mixed signal intensities were observed because of variable intestinal contents (gas, fluid, and

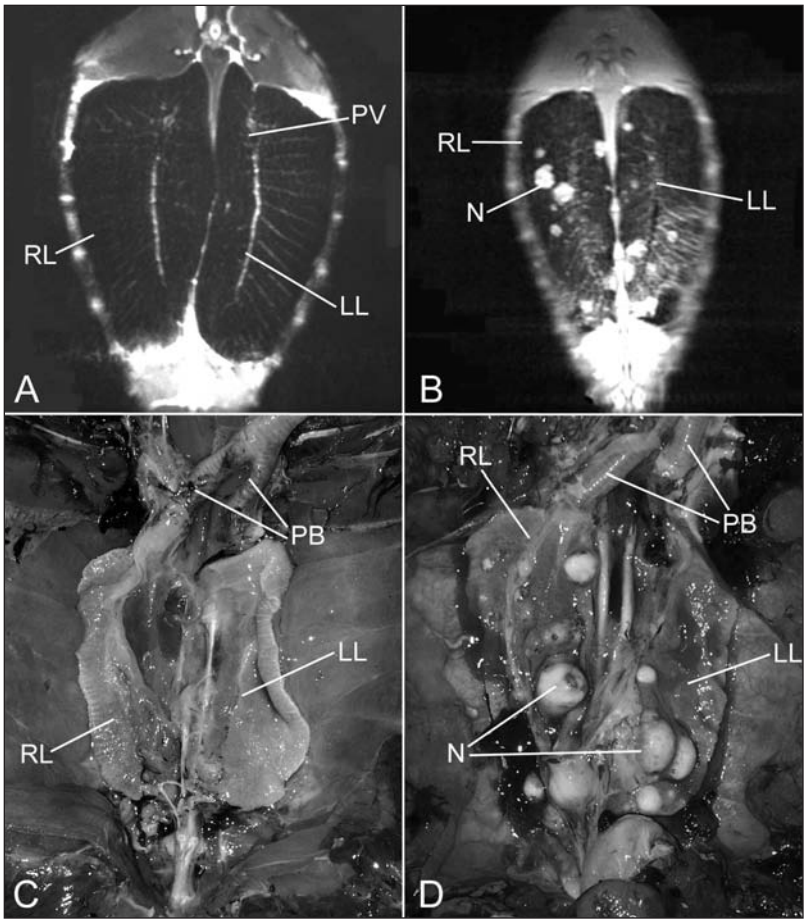

Figure 3—Dorsal plane T2-weighted MR image of the lungs of turtle 8 in which no pulmonary nodules were detected (A); photograph of gross necropsy findings in the same turtle in which the lungs have a normal appearance (C); dorsal plane T1-weighted MR image of the lungs of turtle 5 in which pulmonary fibromas were detected (B); and photograph of gross necropsy findings (multiple nodules in the pulmonary parenchyma; D) in the same turtle. The right side of each MR image and photograph corresponds to the left side of the turtle, and the top of each MR image and photograph corresponds to the cranial end of the turtle. RL = Right lung. LL = Left lung. PV = Pulmonary vasculature. PB = Primary bronchus. N = Nodule.

solid material). Dorsal plane images provided the most complete view of the liver, which was homogeneous and hyperintense compared with skeletal muscle on both T1- and T2-weighted images. On T2-weighted images, the signal intensity of the liver was mildly decreased. The gallbladder could be visualized on both T1- and T2-weighted MR images. Hepatic veins were seen in the hepatic parenchyma and were especially evident on T1-weighted images, where they appeared hypointense compared with surrounding parenchyma. In some instances, the spleen could be seen in the midline, just caudal to the liver on both T1- and T2-weighted images.

The kidneys appeared isointense compared with the liver on T1-weighted images and hyperintense on T2-weighted images (Figure 2). Renal parenchyma appeared fairly homogeneous. The urinary bladder was only detected when it was filled with urine; when empty, it could not be differentiated from adjacent intestine. Gonads were not recognizable on MR images, although it has been reported that ovarian follicles can be seen via MRI in mature chelonians.[6]

Evaluation of turtles with cutaneous fibropapillomatosis—Turtle 2 was found stranded and soon afterwards developed signs of abnormal buoyancy. External fibropapillomas were evident. No abnormalities were found on whole-body radiographs. Magnetic resonance imaging revealed asymmetry of the lungs; the left lung occupied more space than the right. This finding was interpreted as either hyperinflation of the left lung, or pulmonary disease or atelectasis (or both) affecting the right lung. Fluid was detected in the coelomic cavity. Subsequently, a bronchoalveolar lavage was performed, and *Corynebacterium* spp were cultured from the lavage fluid. The turtle was treated with appropriate antimicrobial drugs, and because of the lack of evidence of internal tumors, was released to the wild when treatment was completed.

Turtle 3 was evaluated because it had multiple cutaneous fibropapillomas on the forelimbs and signs of abnormal buoyancy. Whole-body radiographs revealed opacity of both lungs that was more severe in the right lung. Differential diagnoses included diffuse interstitial pneumonia or atelectasis. Magnetic resonance imaging revealed free gas in the coelom, more so on the right side. Small nodules were detected in the caudal portion of the left lung. At necropsy, fibromas were found on the skin; in the eyes, stomach (0.2 to 1.5 cm in diameter), and kidneys (0.2 to 0.7 cm in diameter, on the surface and in the cortex); and in left (0.3 to 0.8 cm in diameter) and right lungs (0.2 to 0.4 cm in diameter).

Turtle 4 was found stranded and had numerous cutaneous fibropapillomas. After excision of fibropapillomas, several recurred. On whole-body radiographs, numerous nodules (7 to 10 mm in diameter) were detected in the pulmonary parenchyma (**Figure 4**). On T1- and T2-weighted MR images, multiple nodules approximately 1 cm in diameter were distributed throughout the lungs. At necropsy, small to medium-sized white nodules were found protruding from the serosal surface of the lungs and within the parenchyma.

Turtle 5 had numerous small cutaneous fibropapillomas. Pulmonary fibromas were detected via radiography at the Turtle Hospital. The diagnosis was confirmed via endoscopy. On MR images, numerous pulmonary nodules ranging from 2 mm to 2.5 cm in diameter were detected in the left and right lung fields (Figure 3). At necropsy, multiple pigmented nodules in both lungs and white raised proliferative lesions that protruded from the gastric mucosa into the lumen were found.

Turtle 6 was found floating at sea. Multiple fibropapillomas were found, and those on the eyes and fore-

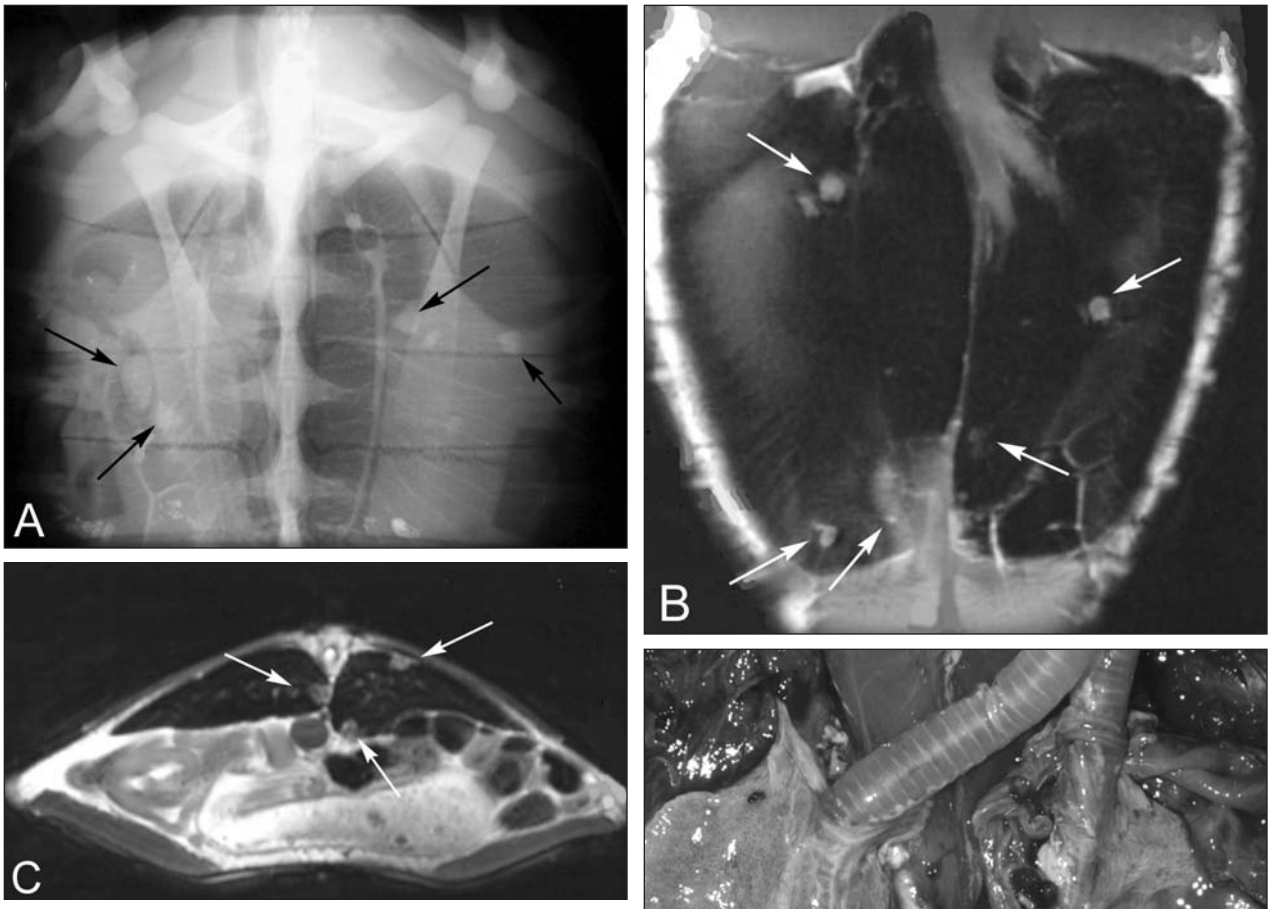

Figure 4—Dorsoventral radiographic view (A), dorsal (B) and transverse plane (C) T2-weighted MR images, and photograph of gross necropsy findings (D) of turtle 4 in which pulmonary fibromas were found. The right side of the radiograph, MR images, and photograph correspond to the left side of the turtle; the top of the radiograph, dorsal plane MR image, and photograph correspond to the cranial end of the turtle. The top of the transverse plane MR image corresponds to the dorsal surface of the turtle. Pulmonary nodules are indicated by arrows.

limbs were removed. Bacterial cellulitis developed at the sites of tumor removal and progressed to osteomyelitis necessitating amputation of the distal portions of the forelimbs. On whole-body radiographs, gas in the subcutaneous tissue of the right antebrachium was detected. The distal phalanges were absent in both forelimbs, and mild soft tissue swelling of the limbs was evident. On MR images, 2 nodules (5 to 10 mm in diameter) were detected in the right lung. The turtle was euthanatized, and at necropsy multiple, variably sized, white nodules were found in both lungs. Multiple raised white nodules on the mucosal surface of the stomach and 1 small white nodule in the liver were found. The lower portion of the gastrointestinal tract had multiple polyps extending from the mucosal surface.

Turtle 7 had 2 cutaneous fibropapillomas. No abnormalities were found on whole-body radiographs (**Figure 5**). Magnetic resonance imaging revealed several small nodules (2 to 5 mm in diameter) distributed throughout the lung field. The stomach contained a mixed-intensity, irregularly marginated, mural mass that partially obscured the gastric lumen. A bicameral fluid-filled mass was observed in the left caudal aspect of the coelom and, compared with the liver, had a hyperintense center surrounded by a hypointense ring on T2-weighted images. The tissue of origin was not clearly recognizable, but kidney or urinary bladder was considered. On the basis of MRI findings, the turtle

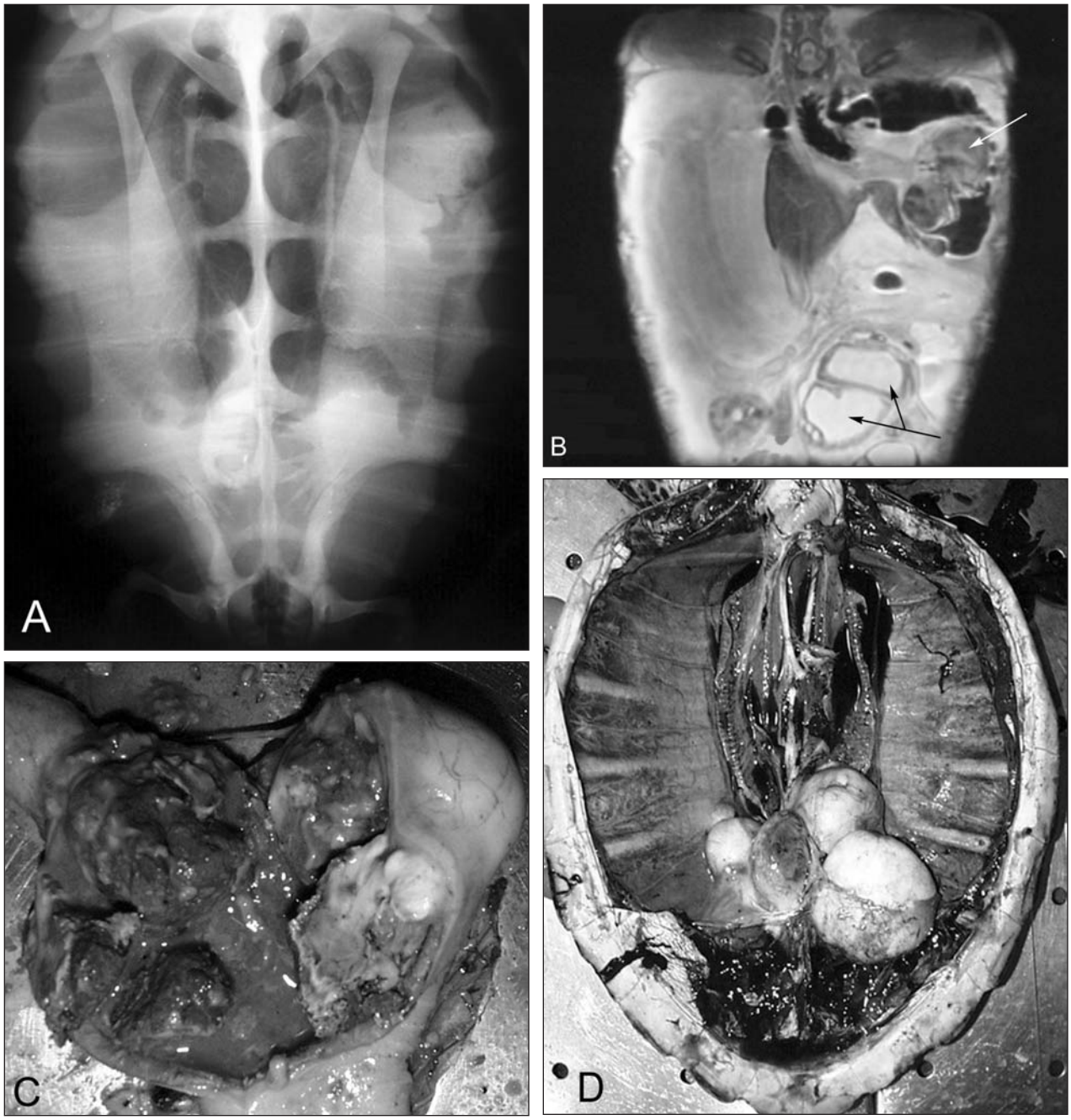

Figure 5—Dorsoventral radiographic view (A), dorsal plane T2-weighted MR image (B), and photographs of necropsy findings (gastric mass, C; and caudal coelomic mass, D) of turtle 7. The right side of the radiograph, MR image, and photographs correspond to the left side of the turtle; the top of the radiograph, MR image, and photographs correspond to the cranial end of the turtle. No abnormalities were found on whole-body radiographs. A space-occupying mass (single arrow) in the stomach and a fluid-filled mass (double-headed arrow) with 2 compartments in the caudal portion of the coelom were detected via MRI.

was euthanatized. At necropsy, 1 small tumor was found in the caudal portion of the left lung. A large fibroma with necrotic areas was found in the stomach. An 8 × 8-cm mass was present in the caudal portion of the coelom and consisted of 2 fluid-filled tumors that appeared to originate from the urinary bladder.

Turtle 8 was found swimming in circles. Cutaneous fibropapillomas were present on the neck and proximal portions of the forelimbs. On whole-body radiographs, an interstitial pattern was evident in both lung fields; no pulmonary nodules were detected. No abnormalities were detected via MRI. The turtle was subsequently found dead and was necropsied. Necropsy revealed fluid trapped in the coelomic mesenteries and severe edema of muscles, fat, and viscera (especially the intestines and kidneys). Multifocal small (2 to 3 mm in diameter) white foci were found in the urinary bladder. Evidence of musculoskeletal trauma over the pelvic girdle with spinal cord compression at the last vertebral scute was detected. A band of

necrotic tissue, which appeared after a traumatic wound to the right dorsal skull, extended into the right olfactory lobe and cerebral cortex. No internal fibromas were found.

Turtle 9 was brought to the Turtle Hospital because of a shell injury. Large cutaneous fibropapillomas were present bilaterally in the axillary and inguinal regions. On whole-body radiographs, several lobulated masses with irregular margins superimposed over the periphery of the carapace, adjacent to the left and right shoulder joints, were evident. Similar masses were seen on the caudal aspect, superimposed over the pelvic and hind limb region. The masses were of soft tissue density and consistent with fibropapillomas seen grossly. On MR images, mixed-intensity irregularly marginated cutaneous masses at both cranial and caudal aspects of the turtle, adjacent to the limbs, were detected. No evidence of nodules in pulmonary or extrapulmonary tissues was detected. Because there was no evidence of internal fibromas, this turtle was eventually released to the wild.

In the 8 turtles with cutaneous fibropapillomatosis, pulmonary nodules were detected in 2 via radiography. On MR images, multiple pulmonary nodules were detected in 5 turtles, and in 1 turtle, internal nodules in other organs were detected. On the basis of these findings, the 5 turtles were euthanatized, and necropsies were performed. All 5 turtles had pulmonary nodules that were diagnosed via histologic examination as fibromas. Of the 5 necropsied turtles, 4 had either multifocal small nodules that protruded above the mucosal surface or more diffuse irregular proliferations in the stomach. None of the gastrointestinal tract abnormalities were detected via radiography, and a gastric mass was apparent on MR images in only 1 of the affected turtles. One small liver nodule in 1 turtle and multiple small nodules in the renal parenchyma of another turtle were found at necropsy. These nodules were not detected via radiography or MRI. One large fluid-filled mass in the caudal portion of the coelom adjacent to the urinary bladder was not evident on whole-body radiographs but was detected via MRI.

Discussion

Comparison of transverse plane MR images of a healthy green turtle with corresponding gross anatomic sections made in the transverse plane revealed that MRI provides a detailed depiction of internal anatomy. Most organs could not be identified on whole-body radiographs; however, most were identified on MR images. These included the lungs, heart, stomach, right and left liver lobes, gallbladder, intestines, and kidneys. The gonads and empty urinary bladder could not be identified in either gross transverse sections or on MR images. The spleen was evident on MR images of 1 turtle. The inability to identify these organs via MRI is likely the result of their small size relative to the MRI slice thickness (4 to 7 mm in the dorsal plane; 5 to 10 mm in the transverse plane). Because all turtles examined in our study were immature, identification of gonads was difficult even at necropsy. The 1 notable difference between the gross anatomic cross-sections and the transverse plane MR images was the relative size of the lung field. In the cadaveric sections, the lungs were small as a result of postmortem collapse; MRI was performed on live turtles with fully inflated lungs.

In our study, pulmonary nodules were detected on survey radiographs in 2 of 8 green turtles with cutaneous fibropapillomatosis. Barnacles, or other objects adhered to the shell, often confounded the detection of internal nodules on radiographs. On radiographs, barnacles appear as areas of opacity superimposed over the coelomic cavity. At times, they were difficult to distinguish from internal nodules.

In contrast, pulmonary nodules were detected via MRI in 5 of 8 turtles with cutaneous fibropapillomatosis; 2 of the 5 were turtles with radiographically detected nodules. Although nodules were not detected radiographically in any other organs, MRI revealed an irregular mass in the stomach and a fluid-filled mass in the caudal portion of the coelomic cavity of 1 turtle. The finding of internal nodules via MRI was used as a criterion for euthanasia; this was because of the progressive and untreatable nature of the disease.

At necropsy, nodules were often found to be more numerous and widely distributed throughout the pulmonary parenchyma than on MR images. This difference may have resulted because of the MRI slice thickness necessitated by the large size of the turtles. A fibroma with a diameter less than the thickness of the slices could be missed via MRI.

The use of MRI for the detection of gastrointestinal and other visceral tumors was not as rewarding as for detection of pulmonary nodules. Three of 4 turtles with multiple gastric nodules found at necropsy had no corresponding abnormalities via MRI. Motion artifact secondary to peristalsis may interfere with the radiologist's ability to fully evaluate the gastrointestinal tract. In addition, contents of the gastrointestinal tract at the time of MRI may obscure underlying lesions.[6] A hepatic nodule found in 1 turtle at necropsy was not detected via MRI; the small size of the nodule likely accounted for the lack of detection on MR images. Surrounding intestine may also have obscured the hepatic nodule. Only 1 of 2 tumors associated with the urogenital tract was diagnosed antemortem via MRI. One turtle with renal fibromas had no evidence of nodules on MR images; once again, this was likely the result of the small size of the tumors relative to the thickness of the MRI slices. Evaluation of the urogenital tract via MRI was limited in our study. The large size of some of the turtles made it difficult to image the entire turtle in the field of view set for MRI; therefore, the imaging parameters established for MRI prevented inclusion of the complete caudal portion of the coelomic cavity on MR images of the larger turtles.

During MRI, the relaxation characteristic of tissues is the most important determinant of signal intensity and contrast on the image.[8] The relaxation characteristic depends on molecule size and the ratio of free-to-bound water in a given tissue. For T1 relaxation time, small molecules, including water, relax much more slowly than medium-sized molecules such as lipids; the T1 relaxation time for protein-bound

water is much shorter than that of free water. As T1 relaxation time decreases, signal intensity (image whiteness) increases.[8] In contrast, the T2 relaxation time increases as bound water is released. Longer T2 relaxation times are associated with more intense signals and whiter images.[8] Therefore, T1-weighted images have opposite contrast effects among tissues than T2-weighted images. In all 5 turtles with pulmonary fibromas, nodules were easily detected on both T1- and T2-weighted images; nodules were roughly circular areas that were hyperintense compared with surrounding pulmonary parenchyma. Nodules were distinguished from bilaterally symmetrical pulmonary vessels, which often had a similar appearance. The other internal nodules detected via MRI were also detected on both T1- and T2-weighted images. However, the fluid-filled tumor in the caudal portion of the coelom of 1 turtle was more easily detected on T2-weighted images because the fluid had a hyperintense (whiter) appearance.

On the basis of the results of our study, it appears that survey radiographs can serve as useful initial screening tools for detection of internal nodules in sea turtles with cutaneous fibropapillomatosis. Radiography is relatively quick, easy, and inexpensive compared with MRI. Radiographs are also necessary to ensure that the turtle is free of metallic objects prior to MRI.[6] In our study, MRI had greater than twice the sensitivity (5 vs 2 turtles) of radiography for the diagnosis of internal fibromas, especially in the lungs. The ability to detect other internal visceral tumors by use of MRI was variable and depended on the size of the turtle, the size of the tumor, and the contents of the gastrointestinal tract. Dorsal plane images generally proved to be more useful than those in the transverse plane because a greater portion of the turtle could be examined with less film to evaluate. Identification of anatomic structures was easier on dorsal plane images because anatomic relationships could be better ascertained from a longitudinal view. Because sea turtles are dorsoventrally flattened, dorsal plane images require a substantially reduced scan time, compared with transverse images. Knowledge of green turtle anatomy and the findings on MR images of a healthy green turtle was critical for accurate interpretation of MR images of turtles with visceral fibromas.

[a]Clearwater Marine Aquarium, Clearwater, Fla.
[b]Gyroscan ACS-NT, Philips Medical Systems, Andover, Mass.
[c]General Electric 1.5T Signa, General Electric Medical Systems, Milwaukee, Wis.

References

1. Herbst LH. Fibropapillomatosis of marine turtles. *Ann Rev Fish Dis* 1994;4:389–425.
2. Quackenbush SL, Work TM, Balazs RN, et al. Three closely related herpesviruses are associated with internal fibropapillomatosis in marine turtles. *Virology* 1998;246:392–399.
3. Schumacher J, Toal RL. Advanced radiography and ultrasonography in reptiles. *Semin Avian Exotic Pet Med* 2001;10:162–168.
4. Whitaker BR, Krum H. Medical management of sea turtles in aquaria. In: Fowler ME, Miller RE, eds. *Zoo and wild animal medicine. Current therapy 4*. Philadelphia: WB Saunders Co, 1999;217–231.
5. Campbell TW. Sea turtle rehabilitation. In: Mader DM, ed. *Reptile medicine and surgery*. Philadelphia: WB Saunders Co, 1996;427–436.
6. Straub J, Jurina K. Magnetic resonance imaging in chelonians. *Semin Avian Exotic Pet Med* 2001;10:181–186.
7. Wyneken J. *The anatomy of sea turtles*. Miami: US Department of Commerce NOAA Technical Memorandum NMFS-SEFSC-470, 2001;1–172.
8. Thomson CE, Kornegay JN, Burn RA, et al. Magnetic resonance imaging: a general overview of principles and examples in veterinary neurodiagnosis. *Vet Radiol Ultrasound* 1993;34:2–17.